ISBN: 978-3-95450-247-9 ISSN: 2673-5490 doi: 10.18429/JACoW-IPAC2024-THYD1

COHERENT ELECTRON COOLING PHYSICS FOR THE EIC *

W. F. Bergan†, P. Baxevanis, M. Blaskiewicz, J. Ma, E. Wang, G. Wang, D. Xu
Brookhaven National Laboratory, Upton, NY, USA
N. Wang, Cornell University, Ithaca, NY, USA
J. Qiang, Lawrence Berkeley National Laboratory, Berkeley, CA, USA
G. Stupakov, SLAC National Accelerator Laboratory, Menlo Park, CA, USA
S. Benson, K. Deitrick, Thomas Jefferson National Accelerator Facility, Newport News, VA, USA
J. Conway, C. Gulliford, C. Mayes, N. Taylor, Xelera Research LLC, Ithaca, NY, USA

Abstract

In order to prevent emittance growth during long stores of the proton beam at the future Electron-Ion Collider (EIC), we need to have some mechanism to provide fast cooling of the dense proton beams. One promising method is coherent electron cooling (CeC), which uses an electron beam to both "measure" the positions of protons within the bunch and then apply energy kicks which tend to reduce their longitudinal and transverse actions. In this work, we discuss the underlying physics of this process. We then discuss simulations which constrain the electrons to move only longitudinally in order to perform fast optimizations and long-term tracking of the bunch evolution, and benchmark these results against fully 3D codes. Additionally, we discuss practical challenges, including the necessity of a high-quality electron beam and sub-micron alignment of the electrons and protons.

INTRODUCTION

The electron-ion collider (EIC) is a new collider planned to be built at Brookhaven National Laboratory which will collide electrons with protons or other ions, allowing better understanding of the proton and nuclear structure [1]. In order to minimize loss of experimental data-taking time, it is desirable to store the protons in the hadron storage ring (HSR) for timescales of 10 hours. However, intrabeam scattering (IBS) and beam-beam effects will cause emittance growth on timescales of as little as 2 hours, reducing the luminosity over the course of the store. The integrated luminosity would be significantly improved if we are able to provide some mechanism which would systematically reduce the proton beam emittance, counteracting the growth due to IBS. However, existing cooling methods, such as linac-based conventional electron cooling [2] or microwave stochastic cooling [3, 4] are unable to cool the high-energy dense proton beams planned for the EIC.

One option is to make use of microbunched electron cooling (MBEC) [5], a specific implementation of the ideas of coherent electron cooling (CeC) [6]. A diagram of this setup is shown in Fig. 1. A beam of electrons having the same relativistic gamma as the protons is injected into a straight section of the HSR called the "modulator," where the two beams propagate together. During this time, the protons provide energy kicks to nearby electrons. The two beams are then separated, and the electrons are sent through a series of straights and chicanes which use the microbunching instability to amplify their initial energy modulations and turn them into density modulations. The two beams are brought together again and copropagate through a straight "kicker" section. By making the transit time of a given proton dependent on its initial energy offset, we can arrange for it to arrive ahead or behind of the electron density spike which it had created, and so receive a corrective energy kick. By having non-zero dispersion and/or dispersion derivatives in the kicker and adding a transverse dependence to the protons' transit times, we can cool transversely as well. More details of the process may be found in Ref. [7–9].

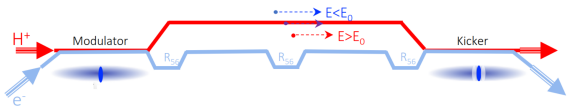

Figure 1: Schematic of microbunched electron cooling.

We describe below extensions to the simple linear theory which are necessary to properly understand and design such a cooling system. We also detail our simulation procedures using a range of codes, as well as an ultimate facility design.

EXTENSIONS TO THEORY

In many regards, CeC may be regarded as an extension of microwave stochastic cooling. Each proton receives a coherent kick due to its own wake, which tends to reduce its action, as well as a random kick due to the wakes of neighboring protons and initial noise in the electron beam, which provides a heating term known as "diffusion." The cooling rate is proportional to the wake amplitude, while the diffusion scales as the square of the wake function, and so sets a limit on the maximum cooling rate achievable. The diffusion term can be reduced by having a shorter wake wavelength, so that a given proton will see the wakes of fewer neighbors. However, in order for cooling to work, the proton must arrive in the kicker near the electrons which it had seen in the modulator, with the length scale also set by the wake wavelength. This imposes strict constraints on the relative alignment of the electron and proton beams, as

* Funded through Department of Energy Offices of Science and Nuclear Physics Contracts DE-SC0012704, DE-AC05-06OR23177, DE-AC03-76SF00515, DE-AC02-05CH11231, DOE SBIR DE-SC0020514, and Graduate Student Research (SCGSR) Program.
† wbergan@bnl.gov

ISBN: 978-3-95450-247-9 ISSN: 2673-5490 doi: 10.18429/JACoW-IPAC2024-THYD1

well as path length differences between individual particles within the beam.

Smearing of Wakes due to Transverse Actions

An important consideration in the design of a cooler is the second-order delay due to the transverse actions of the electrons [10]. Take an electron at longitudinal position s within the lattice. If this electron has transverse angles x' and y', it will arrive at longitudinal coordinate $s + \Delta s$ after travelling a distance $\Delta s\sqrt{1 + x'^2 + y'^2} \approx \Delta s + \frac{x'^2+y'^2}{2}\Delta s$, so that its z coordinate shifts by an amount $\Delta z \approx -\frac{x'^2+y'^2}{2}\Delta s$. Averaging over phases, $\langle x'^2(s)\rangle = J_x\gamma_x(s)$, where J_x is the horizontal action and $\gamma_x(s)$ is the Courant-Snyder gamma function, so that the total delay of a given electron travelling from the modulator at longitudinal coordinate s_M to the kicker at longitudinal coordinate s_K is given by

$$\Delta z \approx -\int_{s_M}^{s_K} \frac{J_x\gamma_x(s) + J_y\gamma_y(s)}{2} ds. \quad (1)$$

Different electrons have different transverse actions, and so will arrive at the kicker at different times. Since the electrons which saw a given proton in the modulator need to also see it in the kicker in order to give it a corrective kick, we need to limit the Courant-Snyder gamma parameters in the electron bypass so that the delay given by Eq. (1) is small relative to the wake wavelength. This in turn limits how small we can make the beta functions in the amplifiers.

Smearing of Wakes due to Energy Offsets

Within the modulator and kicker, a given proton will move longitudinally relative to the electron background due to its fractional energy offset. If this motion is large relative to the wake wavelength, the proton will sample its wake at many locations, providing a smearing effect which reduces the effective wake amplitude.

The size of this effect may be obtained by noting that within a drift of length L, the longitudinal position of the proton will evolve according to $z(s) = z_0 + \frac{\delta}{\gamma^2}s$ for $s \in [-L/2, L/2]$, where δ is the proton's fractional momentum offset, γ is the relativistic gamma, and z_0 is its longitudinal coordinate at the center of the drift. If the wake is modeled as a simple sine wave $w_0(z) = A\sin(kz)$, then performing the longitudinal average over both the modulator and kicker, with respective lengths of L_m and L_k, yields an effective wake function

$$w_{eff}(z) = \frac{\sin(kL_m\delta/2\gamma^2)}{kL_m\delta/2\gamma^2}\frac{\sin(kL_k\delta/2\gamma^2)}{kL_k\delta/2\gamma^2}w_0(z). \quad (2)$$

We also extract an effective off-energy wake from our 1D particle-in-cell (PIC) code, discussed below, modified to allow the source and test proton macroparticles to move within the modulator and kicker straights, respectively, as if they had a given energy offset. These off-energy wakes roughly agree with the theory predictions, with k chosen near the wake wavelength, as shown in Fig. 2. Maintaining short modulator and kicker lengths largely mitigates this effect.

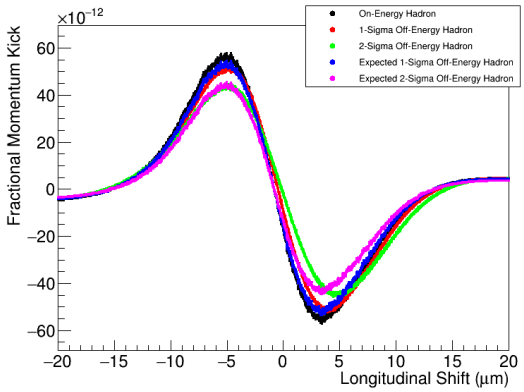

Figure 2: Effective wake function for on- and off-energy 100 GeV protons, both in simulation and rescaled from the on-energy case by Eq. (2). Decent agreement is observed, although there is some additional wake lengthening in the most extreme case.

Longitudinal Alignment

A particularly challenging aspect of the MBEC design is that, after the protons and electrons interact in the modulator, they must be separated, propagate independently for ~100 m, and then rejoin one another so that the protons see the same electrons in the kicker as they had seen in the modulator. The scale for "same" is set by the necessity that any systematic shifts are small relative to the μm-scale wake wavelength [11]. This implies the necessity of maintaining a relative path length stability between the two beams of a few parts per billion, well below what we could hope to measure using conventional diagnostics.

We plan to make use of signal modification, as discussed in Ref. [12]. After the electrons are kicked out of the hadron storage ring at the end of the kicker, the protons continue to propagate for some distance before entering a dipole. The spectral content of the noise in the proton beam at frequencies near the wake wavelength will have been altered by their interaction with the electrons in the kicker, with the exact form of this interaction having a sinusoidal dependence on the relative delays of the two beams. This will alter the intensity of those frequencies in the spectrum of the protons' radiation as they enter a downstream dipole. We expect our signal to take the form of a few parts-per-thousand change in the radiation intensity of the protons at wavelengths of 5 – 30 μm, with emitted power at the wavelengths of interest of at most a few nW, requiring significant detector development.

SIMULATION TOOLS

In order to understand the performance of the cooler, we have set up a long-term tracking code, which tracks the hadrons through a simple lattice including a cooling section.

ISBN: 978-3-95450-247-9 ISSN: 2673-5490 doi: 10.18429/JACoW-IPAC2024-THYD1

Efficiently modeling the cooling section requires knowing the wake function as well as the expected random kick due to diffusion. In this section we discuss how we obtain the wake and diffusion functions in the ideal case, corrections made for saturation and other nonlinear effects, details of the long-term tracking, and the optimization procedure.

Hybrid Wake Functions

In order to have an analytic model for the cooling process (hadron kick to the electrons, amplification, and kick of the electrons to the hadron), we use the method of [13], where the hadrons are treated as point particles in the modulator and kicker, while the electrons are treated as flat rigid discs, which have their charge fall off as Gaussians in the horizontal and vertical directions with RMS sizes equal to the beam size at the relevant location in the lattice. This allows us to use the mathematical tools developed in Ref. [7–9], with the only change being the fact that the H functions, which describe the strength of the hadron-electron interactions in the modulator and kicker, now include a dependence on the transverse hadron position.

In order to benchmark this hybrid wake model, we compare the wakes it obtains to those from the fully 3D models discussed in Ref. [10, 14–16], with the results shown as Fig. 3 for the case of an on-axis, 100 GeV proton at peak electron current. Decent agreement is observed here. However, for off-peak currents, we find that the hybrid model tends to underestimate the wake. Finding a way to efficiently incorporate the 3D wakes into the tracking code will be useful.

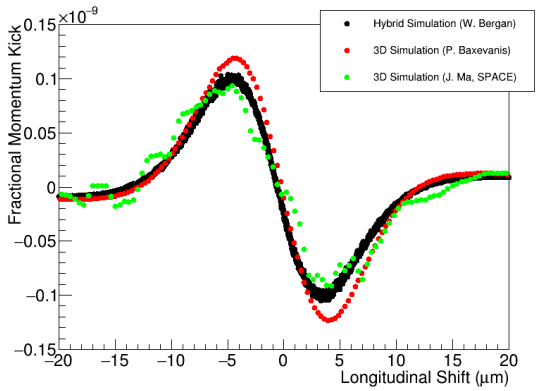

Figure 3: Comparison of the wake for a 100 GeV on-axis proton in the hybrid code as well as two independent 3D codes. Good agreement is observed.

In order to allow for fast evaluation, we use the fit-and-interpolation scheme developed in Ref. [13], both for the wakes and for the diffusion (discussed below).

Diffusion

Diffusion refers to the random momentum kicks which a hadron will receive in the kicker due to the wakes of the neighboring hadrons and electrons. This may be obtained using the method of [17]. For the case where the hadron is to be treated as a point particle, we use the expression for the interaction of a disc-like electron with a point-like hadron in the kicker, as described in Ref. [13], and so we generalize the main result from [17], using the same notation, but with the wake functions modified to depend on the hadron's coordinates in the kicker:

$$\left\langle \Delta\eta^2_{(k,h)}(\vec{x}_k) \right\rangle = \left(\frac{r_h}{\gamma}\right)^2 \int_{-\infty}^{\infty} dz' \Big(n_h w_h^2(\vec{x}_k, z') + n_e w_{e,1}^2(\vec{x}_k, z') + n_e w_{e,2}^2(\vec{x}_k, z') + 2n_e \int_{-\infty}^{\infty} d\eta \frac{1}{\sqrt{2\pi}\sigma_\eta} e^{-\eta^2/2\sigma_\eta^2} \times w_{e,1}(\vec{x}_k, z') w_{e,2}(\vec{x}_k, z' - R_1\eta) \Big). \quad (3)$$

Nonlinear Correction

The above theory assumes that the system is purely linear, so that the contributions of individual hadrons and electrons can be simply added. However, we have found that achieving optimal cooling performance requires us to significantly amplify the wake, to the point that we are close to the saturation limit. In this case, the linear theory starts to break down. We turn to simulation to determine the size of this effect.

For this purpose, we use a 1D particle-in-cell (PIC) code, extended from the one described in Ref. [18]. The main addition from our previous version is the inclusion of the transverse smearing discussed previously: we assign each electron macroparticle horizontal and vertical actions, J_x and J_y, and give them additional delays at each longitudinal step $\Delta z = -\frac{J_x\gamma_x + J_y\gamma_y}{2}\Delta s$. We assume that $\gamma_{x,y}$ are constant in each straight section and set them equal to $3/\beta_{x,y}$ due to necessarily having the Courant-Snyder $\alpha_{x,y} > 1$. The resulting wake is shown in Fig. 4.

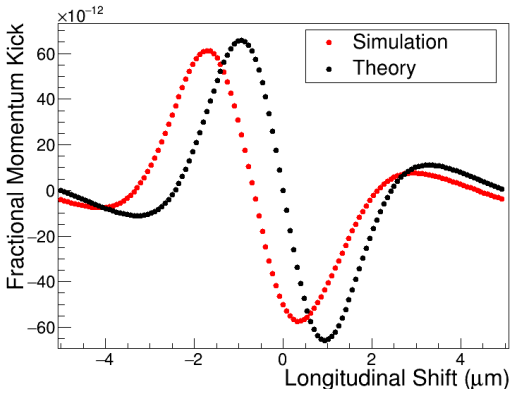

Figure 4: 275 GeV proton wake from simulation compared to that from theory. The amplitudes are similar, but the delays of the electrons due to their transverse actions shift the simulated wake. This effect can be easily corrected by shifting the overall transit time of the electrons or protons.

A key component of extracting the wake function from simulation is the subtraction scheme, where we run the simulation twice with the same noise, but put an additional hadron

ISBN: 978-3-95450-247-9 ISSN: 2673-5490 doi: 10.18429/JACoW-IPAC2024-THYD1

macroparticle at the origin in the second run [10,18–20]. We claimed that taking the difference between these two runs and averaging over noise seeds would give the coherent part of the wake, but it is not obvious that it would give something useful in the nonlinear regime where we operate, since, by definition, the total is not the sum of its parts. However, taking a broader view, we can define a probability density function $P(\Delta\delta; \vec{x}_m, \vec{x}_k, Q)$, which gives the probability that a hadron macroparticle with phase-space coordinates $\vec{x}_k$ in the kicker will receive a momentum kick $\Delta\delta$ if there is, on top of the random noise, a hadron macroparticle with charge Q and phase-space coordinates $\vec{x}_m$ in the modulator. So long as this is not a truly pathological distribution, the mean momentum kick for any given phase-space coordinates is well-defined, and can be treated as the coherent wake. Averaging over noise samples will give us this coherent part, but will be time-consuming. However, first subtracting off the kick the hadron would have received with the same random noise, but with $Q = 0$ in the modulator is simply subtracting a distribution of mean 0 from the distribution whose mean we want to determine, which will not change the final answer. This is exactly our subtraction scheme; while no promises are made concerning the speed of the convergence, we are statistically guaranteed that the coherent wake we obtain is the unique solution for the specified noise parameters.

Once we have this simulated wake, we obtain a rescaling factor by dividing the slope of the simulated wake by that of the theoretical wake, both computed with disc-like hadrons in the modulator and kicker. Similarly, we obtain a diffusion rescaling factor by dividing the mean squared kick to a hadron in simulation by the mean squared kick in theory.

Multi-Turn Cooling

With the rescaled, hybrid wake and diffusion factors known, we proceed to the long-term tracking, which extends the methods of [21]. We initialize a bunch of hadron macroparticles and track them through a simplified ring consisting of a modulator, kicker, RF cavity, and interaction point (IP), with tracking between elements handled by transfer matrices. At the RF cavity, we apply a z-dependent momentum kick to the hadrons to allow for synchrotron motion. We can also manually add in heating effects due to IBS and beam-beam effects by applying momentum kicks in the three planes sufficient to match expected growth rates [22,23] and remove particles exceeding defined apertures from the distribution. At the IP, we obtain the luminosity by integrating the electron density which the various hadron macroparticles see as they pass through the interaction point, assuming an idealized Gaussian electron beam [24]. We adjust the beta functions at the IP to keep the hadron divergence from becoming too large and to keep the electron beam size equal to that of the hadrons.

As the beam passes through the cooler, we use the coherent wake function derived above to give each hadron a momentum kick based on its longitudinal delay in travelling between modulator and kicker and on its transverse positions in each. Since the hadron will in general have some non-zero angle as it passes through the finite-length modulator and kicker, we average the wakes over the transverse coordinates it samples. Generally, the hadron will not see the peak electron current. Based on the wake equations provided by [8], we reduce the amplitude of the wake for a hadron at longitudinal position z within the electron bunch by a factor

$$A \to A \frac{I_e^2(z)}{I_e^2(0)} \frac{\sin^2\left(\phi_0\sqrt{I_e(z)/I_e(0)}\right)}{\sin^2(\phi_0)}, \tag{4}$$

where $I_e(z)$ is the electron current at a given longitudinal position within the bunch and ϕ_0 is the plasma phase advance within the amplifiers at peak bunch current and average wake wavenumber. To handle multiple real turns being simulated in one timestep, we multiply the coherent kick of the wake by the number of turns per timestep.

Since the typical diffusive kick a hadron receives each turn is small, and since we care about the cumulative effects of many such kicks, we take advantage of the central limit theorem to give each hadron each turn a Gaussian random kick with mean squared value given by Eq. (3), similar to what is done in Ref. [25, 26]. To handle multiple real turns being simulated in a single timestep, the magnitude of the kick is increased by the square root of the number of real turns per timestep, since the noise adds in quadrature. The diffusion rates are scaled relative to the local longitudinal hadron and electron densities at the location of the kicked hadron.

Optimization

In order to optimize the design, we run the multi-turn cooling code for a single step to extract the initial cooling rates. In order to reduce the noise present in the stochastic process, we turn off heating due to the IBS and beam-beam effects and do not simulate the diffusion. Instead, we subtract the analytic diffusion rate from the simulated "pure" cooling rate to obtain a typical total cooling rate. Since we cannot run the full nonlinear simulation, we include penalties for large saturation, plasma oscillations in the modulator or kicker, and smearing of the wake due to the electrons' transverse actions and hadron energy offsets. We constrain the total R_{56} (including contributions from straights) between the modulator and kicker centers to be 0, so that an energy chirp in the electron bunch will not introduce timing errors. In order to elegantly maximize the cooling rates in all three planes simultaneously, we make use of the multi-objective genetic algorithm SPEA2 [27], as implemented by the PISA collaboration [28]. This evolves a population of solutions to a Pareto-optimal front, from which we can choose the solutions which give the best balance of the cooling rates in the three planes, in line with the expected heating rates in each plane. These most promising solutions are fine-tuned manually in order to achieve optimal performance in the long-term tracking simulation.

Current design parameters are shown in Table 1 for 100 and 275 GeV protons, corresponding respectively to the third

ISBN: 978-3-95450-247-9 ISSN: 2673-5490 doi: 10.18429/JACoW-IPAC2024-THYD1

Table 1: Cooling Parameters

Proton Energy	**100 GeV**	**275 GeV**
Modulator and Kicker Lengths (m)	33	33
Amplifier Straight Lengths (m)	49	49
Horizontal/Vertical Proton Betas in Modulator (m)	16.6 / 16.4	21.0 / 19.6
Horizontal/Vertical Proton Dispersion in Modulator (m)	0.0036 / 0.096	0.0019 / 0.067
Horizontal/Vertical Proton Dispersion Derivative in Modulator	0.030 / -0.010	0.030 / -0.0049
Proton Horizontal/Vertical Phase Advance (rad)	3.227 / 4.72	3.162 / 4.44
R56 in Proton Chicane (mm)	4.2	0.95
Electron Bunch Charge (nC)	1	1
Electron Peak Current (A)	10	13
Electron Supergaussian Order	4	4
Electron Fractional Slice Energy Spread	1.0×10^{-4}	5.9×10^{-5}
Electron Normalized Emittance (x/y) (mm-mrad)	2.8 / 2.8	2.8 / 2.8
Horizontal/Vertical Electron Betas in Modulator (m)	20.0 / 20.0	21.4 / 21.4
Horizontal/Vertical Electron Betas in Kicker (m)	29.7 / 4.1	7.9 / 7.9
Horizontal/Vertical Electron Betas in Amplifiers (m)	12.0 / 12.0	4.9 / 4.9
R56 in First Electron Chicane (mm)	23.3	12.0
R56 in Second Electron Chicane (mm)	-16.7	-6.7
R56 in Third Electron Chicane (mm)	-18.2	-6.8
Horizontal/Vertical/Longitudinal Heating Times (hours)	2.0 / 4.0 / 2.5	2.0 / 5.0 / 2.9
Horizontal/Vertical/Longitudinal Initial Cooling Times (hours)	1.8 / 4.5 / 3.2	0.9 / 13.1 / 1.4

and second columns of Table 3.3 in Ref. [1]. Note that the hadron optics are symmetric about the center of the cooler, so the proton kicker parameters are not listed. Although we are still revising the details of our long-term tracking model, and in particular the scaling of the beam-beam growth rate and aperture definitions, we consistently see that microbunched cooling roughly doubles the average luminosity.

FACILITY DESIGN

The effectiveness of microbunched electron cooling depends strongly on the quality of the electron beam. In particular, we require a small electron slice energy spread (since the electrons of an electron beam with finite energy spread will become longitudinally separated after passing through any of the electron chicanes, smearing the wake), a small electron beam emittance and large peak current (since we need high electron density for plasma oscillations in the amplification section and kicks to hadrons in the kicker), relatively flat-top longitudinal bunch profile (we need this high current over a relatively long section of the electron bunch to maximize the number of protons which will have good cooling; analytically, we assume a supergaussian electron distribution), and noise close to Poisson noise (since initial noise in the electron beam also gets amplified by the amplification section, contributing to the diffusive heating). This combination of high beam quality and high current can only be efficiently obtained from an energy recovery linac (ERL), and this forms the basis of our design [29–31]. While detailed linac simulations are ongoing, we appear capable of achieving these parameters [32]. In particular, Fig. 5 shows that the expected noise in the electron bunch after removing an irrelevant low-frequency component is close to Poisson shot noise, as desired [33].

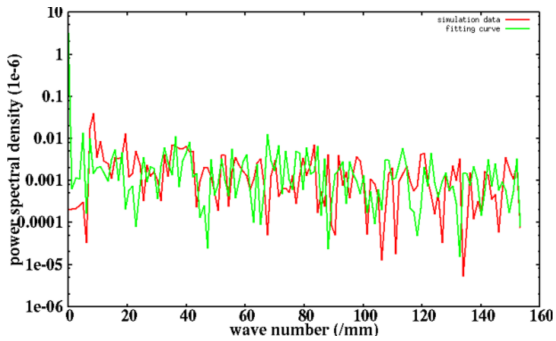

Figure 5: Frequency space electron density distribution at the end of the linac as compared to Poisson shot noise. We have removed a low-frequency component which is outside the acceptance of the amplifier. They are similar, as desired.

CONCLUSION

A fast cooling system is necessary to reach the full physics potential of the EIC. We have discussed the current design status for an MBEC cooler and the range of simulation codes used to understand it. We have also discussed physical effects which must be properly addressed for cooling to work, and how we plan to do so. We are continuing work to address remaining challenges, including longitudinal alignment.

ACKNOWLEDGMENTS

We would like to thank F. Willeke for his support of the cooling efforts, and Y. Luo, V. Ptitsyn, and C. Montag for useful discussions.

ISBN: 978-3-95450-247-9 ISSN: 2673-5490 doi: 10.18429/JACoW-IPAC2024-THYD1

REFERENCES

[1] Electron-ion collider at Brookhaven National Laboratory, conceptual design report 2021, https://www.bnl.gov/EC/files/EIC_CDR_Final.pdf

[2] S. Nagaitsev *et al.*, "Experimental demonstration of relativistic electron cooling", *Phys. Rev. Lett.*, vol. 96, p. 044801, 2006. doi:10.1103/PhysRevLett.96.044801

[3] S. van der Meer, "Stochastic cooling and the accumulation of antiprotons", *Rev. Mod. Phys.*, vol. 57, p. 689, 1985. doi:10.1103/RevModPhys.57.689

[4] M. Blaskiewicz, J. M. Brennan, and F. Severino, "Operational stochastic cooling in the relativistic heavy-ion collider", *Phys. Rev. Lett.*, vol. 100, p. 174802, 2008. doi:10.1103/PhysRevLett.100.174802

[5] D. Ratner, "Microbunched Electron Cooling for High-Energy Hadron Beams", *Phys. Rev. Lett.*, vol. 111, p. 084802, 2013. doi:10.1103/PhysRevLett.111.084802

[6] V. N. Litvinenko and Ya. S. Derbenev, "Coherent electron cooling", *Phys. Rev. Lett.*, vol. 102, p. 114801, 2009. doi:10.1103/PhysRevLett.102.114801

[7] G. Stupakov, "Cooling rate for microbunched electron cooling without amplification", *Phys. Rev. Accel. Beams*, vol. 21, p. 114402, 2018. doi:10.1103/PhysRevAccelBeams.21.114402

[8] G. Stupakov and P. Baxevanis, "Microbunched electron cooling with amplification cascades", *Phys. Rev. Accel. Beams*, vol. 22, p. 034401, 2019. doi:10.1103/PhysRevAccelBeams.22.034401

[9] P. Baxevanis and G. Stupakov, "Transverse dynamics considerations for microbunched electron cooling", *Phys. Rev. Accel. Beams*, vol. 22, p. 081003, 2019. doi:10.1103/PhysRevAccelBeams.22.081003

[10] J. Ma, *et al.*, "Simulation studies of modulator for coherent electron cooling", *Phys. Rev. Accel. Beams*, vol. 21, p. 111001, 2018.

[11] S. Seletskiy, A. Fedotov, and D. Kayran, "Circular attractors as heating mechanism in coherent electron cooling", *Phys. Rev. Accel. Beams*, vol. 25, p. 054403, 2022.

[12] W. F. Bergan, M. Blaskiewicz, and G. Stupakov, "Schottky signal modification as a diagnostic tool for coherent electron cooling", *Phys. Rev. Accel. Beams*, vol. 25, p. 094401, 2022.

[13] W. F. Bergan and G. Stupakov, "Effects of Transverse Dependence of Kicks in Simulations of Microbunched Electron Cooling", in *Proc. NAPAC'22*, Albuquerque, NM, USA, Aug. 2022, pp. 780–783. doi:10.18429/JACoW-NAPAC2022-WEPA67

[14] P. Baxevanis, "3D theoretical and simulation tools for microbunched cooling", technote BNL-222168-2021-TECH, EIC-ADD-TN-021, 2021.

[15] P. Baxevanis, "Generalized wakefield of a microbunched electron cooler", technote BNL-225174-2024-TECH, EIC-ADD-TN-081, 2023.

[16] K. Yu and R. Samulyak, "SPACE Code for Beam-Plasma Interaction", in *Proc. IPAC'15*, Richmond, VA, USA, May 2015, pp. 728–730. doi:10.18429/JACoW-IPAC2015-MOPMN012

[17] W. F. Bergan, "Electron diffusion in microbunched electron cooling", 2024. doi:10.48550/arXiv.2403.17721

[18] W. F. Bergan, "Plasma Simulations for an MBEC Cooler for the EIC", in *Proc. IPAC'21*, Campinas, Brazil, May 2021, pp. 1823–1826. doi:10.18429/JACoW-IPAC2021-TUPAB180

[19] Y. Jing, V. N. Litvinenko, Y. Hao, and G. Wang, "Model Independent Description of amplification and saturation using Green's Function", 2015. doi:10.48550/arXiv.1505.04735

[20] A. Al Marzouk and B. Erdélyi, "Collisional simulations of the modulator section in coherent electron cooling", *Phys. Rev. Accel. Beams*, vol. 27, p. 044401, 2024.

[21] W. F. Bergan, P. Baxevanis, M. Blaskiewicz, G. Stupakov, and E. Wang, "Design of an MBEC Cooler for the EIC", in *Proc. IPAC'21*, Campinas, Brazil, May 2021, pp. 1819–1822. doi:10.18429/JACoW-IPAC2021-TUPAB179

[22] J. D. Bjorken and S. K. Mtingwa, "Intrabeam scattering", *Part. Accel.*, vol. 13, pp. 115-143, 1983.

[23] S. Nagaitsev, "Intrabeam scattering formulas for fast numerical evaluation", *Phys. Rev. ST Accel. Beams*, vol. 8, p. 064403, 2005. doi:10.1103/PhysRevSTAB.8.064403

[24] A. W. Chao, K. H. Mess, M. Tigner, and F. Zimmermann, *Handbook of Accelerator Physics and Engineering*, 2nd Ed., Singapore: World Scientific, 2013.

[25] G. Wang, "Evolution of ion bunch profile in the presence of longitudinal coherent electron cooling", *Phys. Rev. Accel. Beams*, vol. 22, p. 111002, 2019.

[26] S. T. Wang *et al.*, "Simulation of the transit-time optical stochastic cooling process in the Cornell Electron Storage Ring", *Phys. Rev. Accel. Beams*, vol. 24, p. 064001, 2021.

[27] E. Zitzler, M. Laumanns, and L. Thiele, "SPEA2: improving the Strength Pareto Evolutionary Algorithm for multiobjective optimization", in *Proc. EUROGEN2001*, Athens, Greece, Sep. 2001, pp. 95–100.

[28] S. Bleuler, M. Laumanns, L. Thiele, and E. Zitzler, "PISA — A platform and programming language independent interface for search algorithms", in *Proc. 2nd Int. Conf. on Evolutionary Multi-Criterion Optimization (EMO'03)*, Faro, Portugal, Apr. 2003, pp. 494–508.

[29] E. Wang *et al.*, "The Accelerator Design Progress for EIC Strong Hadron Cooling", in *Proc. IPAC'21*, Campinas, Brazil, May 2021, pp. 1424–1427. doi:10.18429/JACoW-IPAC2021-TUPAB036

[30] E. Wang *et al.*, "Electron Ion Collider Strong Hadron Cooling Injector and ERL", in *Proc. LINAC'22*, Liverpool, UK, Aug.-Sep. 2022, pp. 7–12. doi:10.18429/JACoW-LINAC2022-MO2AA04

[31] K. Deitrick *et al.*, "Development of an ERL for coherent electron cooling at the Electron-Ion Collider", in Proc. IPAC'24, Nashville, TN, USA, May 2024, paper THPC46.

[32] E. Wang, W. Bergan, S. Benson, and J, Qiang, "Generating supergaussian distribution and uniform sliced energy spread bunch for EIC strong hadron cooling", in Proc. IPAC'24, Nashville, TN, USA, May 2024, paper MOPC24.

[33] J. Qiang and E. Wang, "Simulation of shot noise effects in the EIC strong hadron cooling accelerator using real number of electrons", in *Proc. IPAC'23*, Venice, Italy, May 2023, pp. 2743–2746. doi:10.18429/JACoW-IPAC2023-WEPA041